ELSEVIER

Ecological Modelling 164 (2003) 211–226

ECOLOGICAL MODELLING

www.elsevier.com/locate/ecolmodel

Modelling the impacts of the foliar pathogen, *Phaeocryptopus gaeumannii*, on Douglas-fir physiology: net canopy carbon assimilation, needle abscission and growth

Daniel K. Manter [a,*], Barbara J. Bond [a], Kathleen L. Kavanagh [b], Jeffrey K. Stone [c], Gregory M. Filip [a]

[a] *Department of Forest Science, Oregon State University, Corvallis, OR 97331, USA*
[b] *Forest Resources Department, University of Idaho, Moscow, ID 83844, USA*
[c] *Botany and Plant Pathology Department, Oregon State University, Corvallis, OR 97331, USA*

Received 27 March 2002; received in revised form 7 October 2002; accepted 5 December 2002

Abstract

This paper describes the parameterisation, testing and implementation of needle-level stomatal conductance (g_s) and net CO_2 assimilation (A_{net}) models that include the physiological impacts of the Douglas-fir pathogen, *Phaeocryptopus gaeumannii*. Hourly estimates of g_s were modelled by assuming that stomata regulate water flux such that plant water potential is maintained above a critical threshold, and A_{net} was modelled based on the kinetics of photochemistry. The model was tested using summer field measurements from trees at three western Oregon Douglas-fir (*Pseudotsuga menziesii*) plantations with varying levels of *P. gaeumannii*, and showed a high degree of accuracy: $r^2 = 0.777$ and 0.792 for g_s and A_{net}, respectively. Instantaneous needle-level estimates of g_s and A_{net} were also scaled-up to a whole-canopy estimate for a 10-month period (July 1998–April 1999). At all three sites, a significant seasonality in A_{net} was observed, with the highest rates occurring during the summer months (up to 400 g CO_2 m^{-2} LA) declining to near or below zero during the winter. The presence of *P. gaeumannii* had a significant impact on needle- and whole-canopy A_{net}, and for the needle age classes where colonisation levels reached 25% pseudothecia density (i.e. percent of stomata with visible fruiting bodies), estimated total carbon budgets were negative. However, at the whole-canopy level all trees maintained a positive carbon budget due to the large contribution from current year needles that remain unaffected by the fungus for the first 6 months of development, or until the emergence of pseudothecia. Furthermore, the abscission of the older, more-heavily diseased foliage, shortly after becoming a carbon sink, has a significant mitigating effect on whole-canopy A_{net}. For example, at the high-disease site, *P. gaeumannii*-associated reductions in A_{net} per unit leaf were estimated to reduce whole-canopy A_{net} by ca. 110% without needle abscission, but this was reduced to 85% when older, more-heavily diseased needles were abscised.

Keywords: Gas exchange; Needle longevity; Nitrogen; Plant-pathogenic fungi; *Pseudotsuga menziesii*; Rubisco; Stomatal conductance

1. Introduction

Douglas-fir (*Pseudotsuga menziesii*) forest plantations are some of the most productive in the world (McMurtrie, 1993), with over 15 million ha currently

* Corresponding author. Present address: USDA Forest Service, Pacific Northwest Research Station, Forestry Sciences Laboratory, 3200 Jefferson Way, Corvallis, OR 97331, USA.
Tel.: +1-541-758-7768; fax: +1-541-758-7760.
E-mail address: dmanter@fs.fed.us (D.K. Manter).

0304-3800/03/$ – see front matter © 2003 Elsevier Science B.V. All rights reserved.
doi:10.1016/S0304-3800(03)00026-7

in production (Hermann and Lavender, 1999). However, over the past 10 years, Swiss needle cast disease (SNC), caused by the parasitic foliar fungus, *Phaeocryptopus gaeumannii*, has intensified in forest plantations of the Pacific Northwest of the United States (PNW). The area affected by SNC increased from 52,600 to 119,500 ha between 1996 and 1999 (Hansen et al., 2000), potentially limiting the productivity of these stands. Indeed, volume growth has recently been reported to be 23–50% less than expected in these PNW forest plantations (Maguire et al., 2002); however, it is unknown if SNC is responsible for the observed growth losses. Historically, *P. gaeumannii* has been considered a weak pathogen with limited impact on tree growth (Boyce, 1940; Hood, 1982); however, given the current accelerated rates of fungal development i.e. fruiting occurring on current year (Hansen et al., 2000) rather than 3- or 4-year-old needles (Boyce, 1940; Hood, 1982) and recent elucidation of the mechanism of *P. gaeumannii*'s impact on Douglas-fir physiology (Manter et al., 2000), we chose to quantify the potential influence of *P. gaeumannii* on whole-tree physiology and growth using a modelling approach.

The objective of this study was to parameterize and test a model of Douglas-fir net CO_2 assimilation with varying levels of *P. gaeumannii* colonisation. Once validated, this model could then be used to determine: (i) the impact of *P. gaeumannii* on Douglas-fir physiology at larger time and spatial scales, (ii) if *P. gaeumannii*'s impact is correlated with the current growth losses in coastal Oregon Douglas-fir plantations—testing the hypothesis that SNC is responsible for the observed growth losses, and (iii) the impact as disease level increases or decreases.

2. Model development and testing

2.1. Plant material

The plant material necessary for estimation of model parameters consisted of Douglas-fir seedlings and field trees from two separate studies. The field trees consisted of 12–15-year-old trees from three western Oregon plantations. Two of the plantations are located in the Coast Range (i.e. Beaver and Hebo), and these sites have severe and moderate levels of *P. gaeumannii* infection, respectively. The third plantation is from the Willamette Valley with low levels of *P. gaeumannii* infection (i.e. Mac). At each site, paired permanent plots were created on north- and south-facing slopes (10–30%), and within each plot six infected (i.e. no spray) trees and six uninfected (i.e. spray) control trees were measured. Control trees were kept disease-free by spraying foliage with chlorothalonil (Bravo 720, rate = 66 ml/3.78 l, applied until run-off) by means of a backpack sprayer. Fungicide applications were conducted in 1998 and 1999 at bud break (90% trees had broken bud) and 1 month following bud break.

Two-year-old Douglas-fir seedlings (open-pollinated Oregon north-coast seed source, Starker Forests Inc., Corvallis, OR, USA) with different levels of *P. gaeumannii* infection were also utilised. To vary rates of infection, seedlings were incubated for 2, 4, or 8 weeks in the understory of *P. gaeumannii*-infected trees (Salal plot, see Hansen et al., 2000) from May to July 1999. Except during the inoculation period, all seedlings were stored in a cold frame at the Oregon State University Botany Farm (Corvallis, OR, USA), fertilised with Osmocote Pro 18-8-8 (Scotts-Sierra Horticultural Products Co., Marysville, OH, USA) and irrigated as needed.

2.2. Model parameterisation

Estimates of photobiochemical parameters (e.g. V_{cmax}, maximum rate of carboxylation; J_{max}, maximum rate of electron transport; and R_d, respiration in the presence of light) were calculated from A/C_i curves (i.e. net CO_2 assimilation measured over a range of calculated internal CO_2 concentrations or C_i) according to the model proposed by Farquhar et al. (1980). A LiCor 6400 gas exchange system (LiCor, Inc., Lincoln, NE, USA) was used for these measurements. During measurements, cuvette conditions were maintained at photosynthetic photon flux density (400–700 nm, PPFD) = 2000 μmol m^{-2} s^{-1}, temperature = 25 °C, [H_2O vapor] $\geq$ 14 mmol mol air^{-1}, and flow rate = 100 mmol m^{-2} s^{-1}, unless otherwise noted. A/C_i response curves were measured by varying the cuvette CO_2 concentration, allowing equilibration to a steady state ([CO_2] coefficient of variation < 2%), and logging measurements every 10 s for 1 min. CO_2 was varied in the following order: 40, 30, 20, 60, 80, 100,

120, 160, and 200 Pa. Temperature dependencies photobiochemical parameters were determined from A/C_i curves conducted at air temperatures of 10, 18, 23, 25, 28, 30, and 35 °C following a 45 min equilibration period.

Infection levels of *P. gaeumannii* were estimated by the presence of pseudothecia (i.e. fruiting bodies) emerging from stomata. Values are reported as the percent of stomata occupied with pseudothecia (i.e. pseudothecia density or PD), calculated as the mean value of for each sampled tree based on the sampling procedures outlined in Manter et al. (2000).

Following A/C_i analysis of the field trees (12 per site) in June 1998, 2 g FW of 1-year-old needles adjacent to the cuvette were collected and used to determine total foliar *N* content (% w/w). All analyses were performed by the Central Analytical Laboratory (Crop and Soil Science Department, Oregon State University, Corvallis, OR, USA) using a Leco CNS 2000.

2.3. Model derivation

The needle-level gas exchange model consists of two separate but related processes. First, g_s is calculated assuming that stomatal regulation operates in such a manner as to maintain plant water potential above a threshold level (Bond and Kavanagh, 1999). Second, A_{net} is estimated based on the model proposed by Farquhar et al. (1980).

Several authors (e.g. Jones and Sutherland, 1991; Dewar, 1995; Whitehead, 1998; Bond and Kavanagh, 1999) have suggested that stomatal behavior is dependent on the water supply capacity of the vascular system, and can be described mathematically:

$$g_s \times \mathrm{VPD} = K_L(\Psi_{soil} - \Psi_{leaf}) \quad (1)$$

where g_s is the stomatal conductance (mmol m^{-2} s^{-1}), VPD the leaf-to-air vapor pressure gradient (Pa), K_L the leaf-specific hydraulic conductance (mmol m^{-2} s^{-1} MPa^{-1}), and Ψ_{soil} and Ψ_{leaf} are the water potential of the soil and leaf (MPa), respectively. Estimation of g_s using Eq. (1) was similar to that proposed by Bond and Kavanagh (1999). Calculations were as follows:

Step 1. A maximum stomatal conductance (g_{s_max}) based on the presence of *P. gaeumannii* was calculated using Eq. (2) (adapted from Manter et al., 2000):

$$g_{s\_max} = 150\left(\frac{100-(0.696+1.720 \times \mathrm{PD})}{100}\right) \quad (2)$$

where PD is the percent of stomata occupied with *P. gaeumannii* pseudothecia and 150 is a typical g_{s_max} for Douglas-fir (Bond and Kavanagh, 1999).

Step 2. A preliminary value of Ψ_{leaf} was estimated using a reorganised Eq. (1):

$$\Psi_{leaf} = \Psi_{soil} - \left(\frac{g_{s\_max} \times \mathrm{VPD}}{K_L}\right) \quad (3)$$

Based on the results of water flux studies in Douglas-fir branches (D.K. Manter and K.L. Kavanagh, unpublished data), a *P. gaeumannii*-adjusted whole-tree K_L was calculated as:

$$K_L = (111.9 - 0.976 \times \mathrm{LW}) \times 0.001 \quad (4)$$

where LW is the percent of latewood in each sapwood annual ring, and 0.001 is scaling factor relating branch and whole-tree K_L.

Step 3. If $\Psi_{leaf} < \Psi_{threshold}$
Step 3a. $\Psi_{leaf} = \Psi_{threshold}$
Step 3b. $g_s = K_L(\Psi_{soil} - \Psi_{leaf})/\mathrm{VPD}$

Step 4. If $\Psi_{leaf} > \Psi_{threshold}$
Step 4a. $g_s = g_{s\_max}$

Step 5. A light-limited g_s (g_{s_ppfd}), based on data from Leverenz (1981), was calculated:

$$g_{s\_ppfd} = g_{s\_max}(1 - \exp(-0.017 \times \mathrm{PPFD})) \quad (5)$$

Step 6. Finally, the modelled stomatal conductance (g_{s_model}) was set equal to

$$g_{s\_model} = \min(g_s, g_{s\_ppfd}) \quad (6)$$

The model of photosynthesis is based on the biochemistry model outlined in Farquhar et al. (1980), with some modifications due to the impacts of *P. gaeumannii* infection. As suggested by Farquhar et al. (1980), net CO_2 assimilation can be expressed mathematically as:

$$A = V_c - 0.5 \times V_o - R_d = V_c\left(1 - \frac{0.5 \times O}{\tau C_i}\right) - R_d \quad (7)$$

where V_c and V_o are rubisco carboxylation and oxygenation rates (μmol m^{-2} s^{-1}), respectively. C_i and O are the intercellular partial pressures (Pa) of CO_2 and O_2, R_d the respiration rate (μmol m^{-2} s^{-1}) in the presence of light, and τ (μmol m^{-2} s^{-1}) is the specificity factor for rubisco (Jordan and Ogren, 1984). The rate of V_c is limited by either the rubisco activity (W_c) or electron transport (W_j), therefore Eq. (7) becomes:

$$A = \left(1 - \frac{0.5 \times O}{\tau C_i}\right) \min(W_c, W_j) - R_d \quad (8)$$

$$W_c = \left(\frac{V_{cmax} C_i}{C_i + K_c(1 + O/K_o)}\right) \quad (9)$$

$$W_j = \left(\frac{JC_i}{4(C_i + O/\tau)}\right) \quad (10)$$

$$J = \frac{\alpha I}{(1 + (\alpha^2 I^2 / J_{max}^2))^{0.5}} \quad (11)$$

where V_{cmax} is the maximum rate of carboxylation (μmol m^{-2} s^{-1}), K_c and K_o the Michaelis–Menton constants for carboxylation and oxygenation, respectively, J the rate of electron transport (μmol m^{-2} s^{-1}), α the efficiency of light energy conversion on an incident light basis (mol e$^-$ mol^{-1} absorbed photons) and J_{max} is the maximum rate of electron transport (μmol m^{-2} s^{-1}).

Before proceeding with the photosynthesis estimation procedure several unknown parameters must first be defined (i.e. K_c, K_o, t, R_d, V_{cmax}, and J_{max}). As in Harley et al. (1992) we chose to model K_c, K_o and τ based on the temperature dependencies outlined in Jordan and Ogren (1984) using Eq. (12):

$$\text{Parameter} = \exp\left(\frac{c - \Delta H_a}{RT_k}\right) \quad (12)$$

where c is a scaling constant, ΔH_a an activation energy, R the universal gas constant and T_k is the leaf temperature (K) (see Table 1, Harley et al., 1992). Whereas the temperature dependencies of V_{cmax} and J_{max} can be mathematically expressed as

$$\text{Parameter} = \frac{\exp(c - \Delta H_a / RT_k)}{1 + \exp((\Delta S\, T_k - \Delta H_d)/RT_k)} \quad (13)$$

where ΔH_d is the energy of deactivation and ΔS is an entropy term. All parameter estimates used in Eq. (13) are shown in Fig. 1.

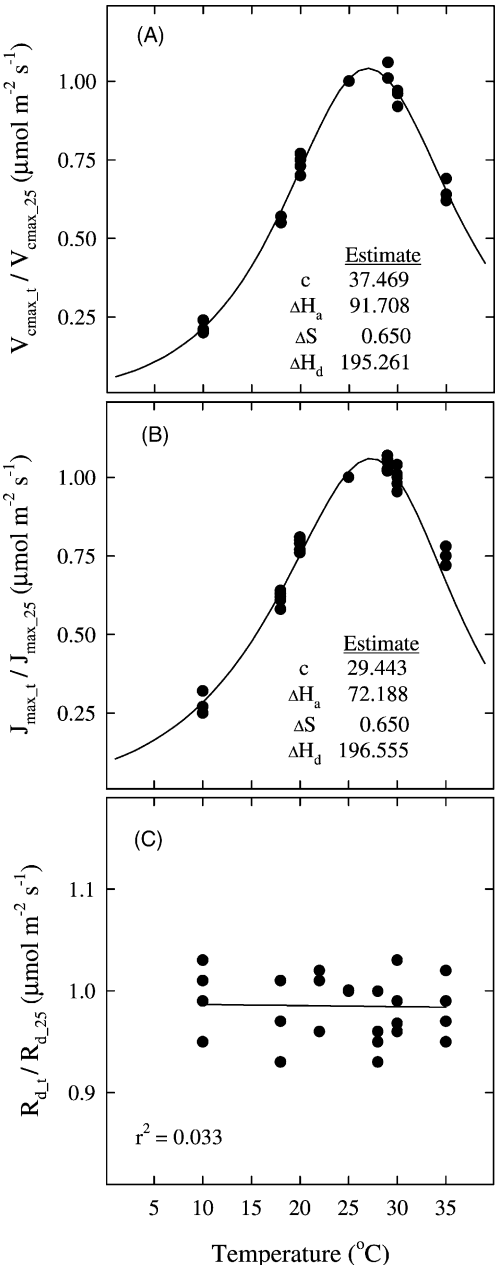

Fig. 1. Temperature dependency of the maximum rates of carboxylation (V_{cmax}) and electron transport (J_{max}), and respiration rate in the presence of light (R_d) for six 2-year-old Douglas-fir seedlings infected with varying amounts of *P. gaeumannii* (i.e. PD was ca. 0, 5, 10, 20, 40 and 50%). Parameters were estimated from A/C_i curves at each air temperature following a 45 min equilibration time using a LiCor 6400. To account for fungal-induced changes, all parameters were normalised by dividing by parameter estimates at 25 °C. Measurements were conducted in April 2000.

Table 1
Observed maximum net CO_2 assimilation (A_{net}, $\mu mol\,m^{-2}\,s^{-1}$) and PD (%) from three western Oregon Douglas-fir plantations

Age class	Mac sites		Hebo sites		Beaver sites	
	A_{net}	PD	A_{net}	PD	A_{net}	PD
Current year	11.0 (1.5) a	0.0 (0.0) x	10.3 (0.9) a	1.5 (0.5) x	8.5 (1.1) a	2.2 (0.6) x
1 year	9.2 (1.3) a	3.1 (2.3) y	7.6 (1.2) b	12.0 (1.4) y	4.9 (0.7) b	24.7 (5.1) y
2 year	10.3 (1.6) a	0.2 (0.1) x	3.8 (0.8) c	18.6 (2.1) z	2.1 (0.4) c	45.0 (6.1) z

Using the four diurnal measurements of gas exchange for each site (June, July, August, and September 1998) an average of maximum A_{net} and PD (pseudothecia density) was calculated for each day from the six un-sprayed trees (north and south plots combined) at each site. Standard errors are in parentheses. For each parameter, means for the 1- and 2-year-old age classes were compared with the current year age class using a paired *t*-test. Means within a column with different letters are significantly different $P \leq 0.05$.

For V_{cmax}, J_{max}, and R_d, a Douglas-fir specific temperature dependency was estimated using the 2-year-old seedlings (Fig. 1). Due to *P. gaeumannii* impacts on V_{cmax} and J_{max} (see Eqs. (14) and (15)), all values for a given seedling (Fig. 1) were normalised by parameter estimates at 25 °C (i.e. V_{cmax_25}, J_{max_25}, and R_{d_25}). In previous studies (e.g. Farquhar et al., 1980; Harley et al., 1992), V_{cmax} has been estimated from leaf nitrogen concentrations. Based on an assessment of this relationship in 1-year-old needles from 36 coastal Oregon Douglas-fir trees (12 from each of the high-, medium- and low-disease plantations), we found no relationship between leaf nitrogen concentration and V_{cmax} (Fig. 2). However, a strong correlation between V_{cmax} and *P. gaeumannii* infection levels was observed (Fig. 3A); therefore, V_{cmax_25} was estimated using Eq. (14):

$$V_{cmax\_25} = 30.641 \times \exp(-0.041 \times PD) \quad (14)$$

Previous studies (e.g. Harley et al., 1992; Wullschleger, 1993) report a strong correlation between V_{cmax_25} and J_{max_25}. In our sample population, a significant relationship was also observed (Fig. 3B), and is defined by Eq. (15):

$$J_{max\_25} = 23.914 + 1.955 \times V_{cmax\_25} \quad (15)$$

Finally, because neither temperature (Fig. 1C, also see Harley et al., 1992) nor *P. gaeumannii* infection level (Fig. 3C) had a significant effect on R_d, R_d was held constant at $1.64\,mmol\,m^{-2}\,s^{-1}$.

All climatic data required for model parameterisation (RH, *T*, and PPFD) were collected using HOBO dataloggers Spectrum Technologies, Inc. (Plainfield, IL, USA). One set of dataloggers was installed at a height of 1.5 m in an opening (radius > 5 m) at each study site. Due to the wide tree spacing, open canopies, and low needle retention in these stands, within-canopy changes in light penetration were negligible and not incorporated into the model. The remaining unknown, and driving variable for the above biochemical equations, is C_i, which results from the interaction of A_{net} and g_s based on the flux equation:

$$C_i = C_a - \frac{A}{g_s} \quad (16)$$

where C_a is the atmospheric CO_2 concentration (assumed to be 35.5 Pa) outside the leaf boundary layer. Due to the interactive effects of A_{net} and g_s on C_i, we cannot estimate C_i independent of A_{net} and g_s.

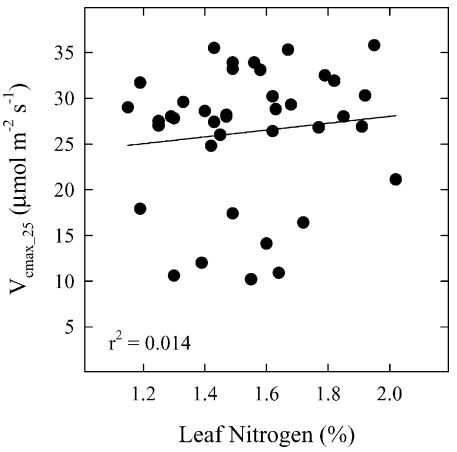

Fig. 2. Relationship between leaf nitrogen concentration and the maximum rate of carboxylation at 25 °C (V_{cmax_25}) in 1-year-old needles from three coastal Oregon Douglas-fir plantations. Six sprayed and six un-sprayed (PD ranged from 0 to 30%) trees were sampled from western Oregon Douglas-fir plantations ($n = 36$). Measurements were conducted in June 1998.

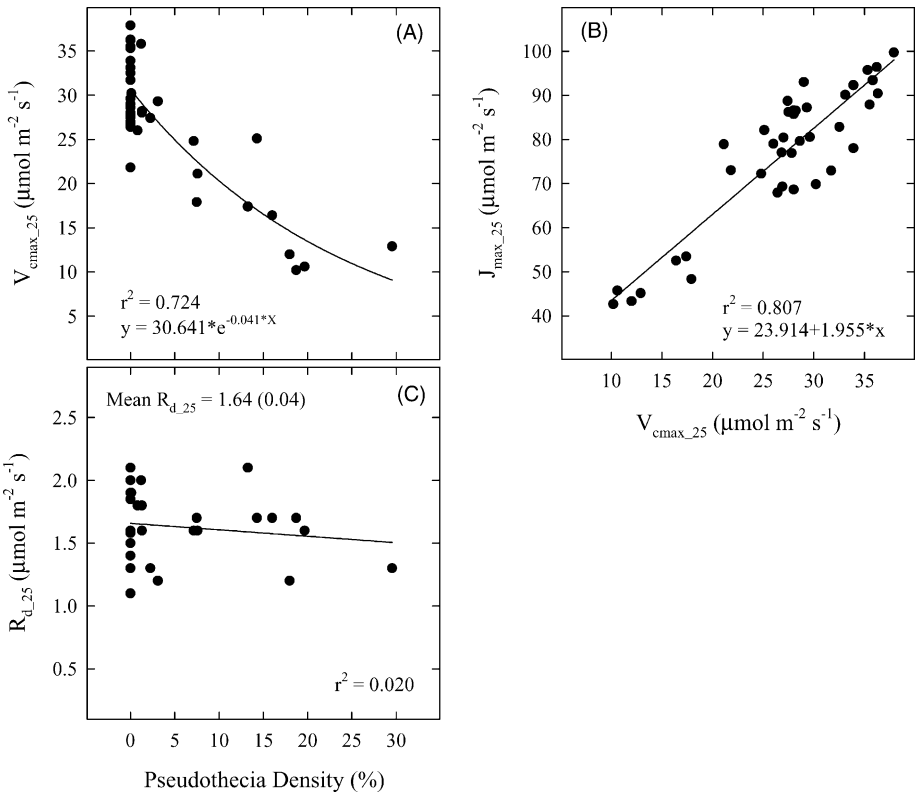

Fig. 3. Relationships used to estimate Farquhar-biochemistry parameters, i.e. the maximum rates of carboxylation (V_{cmax}) and electron transport (J_{max}), and respiration rate in the presence of light (R_d), in 1-year-old needles from three coastal Oregon Douglas-fir plantations. Six sprayed and six un-sprayed (PD) ranged from 0 to 30% trees were sampled from western Oregon Douglas-fir plantations (n = 36). Measurements were conducted in June 1998.

This problem was overcome by first estimating g_s (see stomatal conductance sub-model), then simultaneously solving for the two unknowns (A_{net} and C_i) using Eqs. (8) and (16). For all observations, unique values of A_{net} and C_i were estimated using the model procedure in the SAS statistical package (SAS Institute Inc., Cary, NC, USA).

2.4. Model validation

Model estimates were tested against diurnal gas exchange measurements from at least three diseased and three healthy trees (i.e. sprayed with the fungicide chlorothalonil) at each site. On each sample date, gas exchange was measured on the three youngest needle age classes from one sun-exposed, lower-canopy branch. 1998 measurements of CO_2 and water fluxes were recorded using a LiCor 6200 portable infrared gas exchange analyser, and 1999 measurements consisted of water flux using a LiCor 1600.

Fig. 4 shows a plot of the predicted versus measured stomatal conductance values. Overall, modelled values were highly correlated with observed values (r^2 = 0.777); however, the model tended to slightly underestimate g_s (slope = 0.818). Regression analysis showed that none of the treatments (i.e. site, *P. gaeumannii* infection level, needle age) significantly affected the relationship between observed and predicted g_s values (data not shown). The major limitation of using our model to predict g_s arises from an overestimation of g_s during the mid-morning hours. For example, Fig. 5 depicts a typical diurnal curve for both observed and predicted g_s at a low-disease site (Mac-north). Clearly, observed values of stomatal conductance decline earlier than the modelled values. Two factors may be responsible. First, our estimates

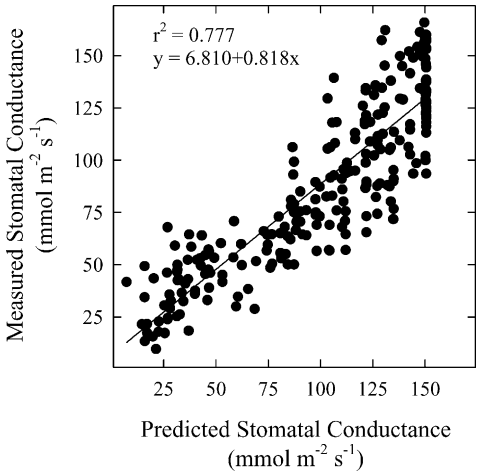

Fig. 4. Measured vs. predicted stomatal conductance (g_s) for current year, 1- and 2-year-old needles with varying levels of *P. gaeumannii* infection (PD) ranged from 0 to 61% from three western Oregon Douglas-fir plantations. Each point is the mean of six trees ($n = 289$) measured in 1998 and 1999.

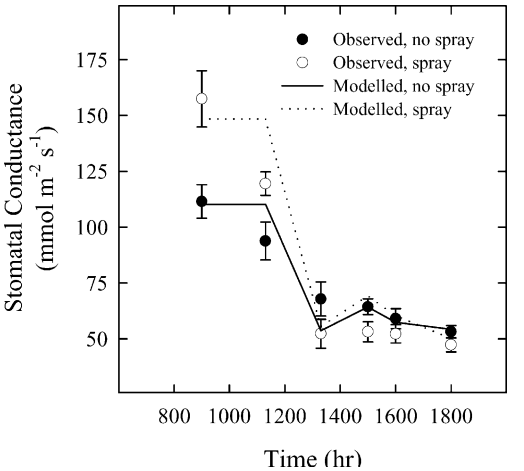

Fig. 6. Diurnal pattern of measured and predicted stomatal conductance (g_s) for sprayed (mean PD was 0%) and un-sprayed (mean PD was 15%) 1-year-old needles from the high-disease site (Beaver-south) on 7 July 1998. Each observation is the mean and standard error for three trees.

of Ψ_{leaf} are based on instantaneous estimates of water loss, which may overestimate Ψ_{leaf} due to the loss of water prior to the current time-step. Second, our model assumes that stomatal closure occurs only at the critical value of Ψ_{leaf} (−2.1 MPa); however, g_s may begin to decline at higher Ψ_{leaf} (Webb, 1991).

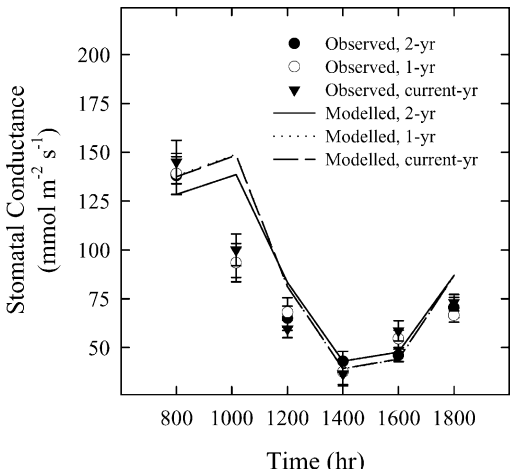

Fig. 5. Diurnal pattern of measured and predicted stomatal conductance (g_s) for sprayed current year, 1- and 2-year-old needles (mean PD was 0, 0 and 4%, respectively) from the low-disease site (Mac-north) on 9 July 1998. Each observation is the mean and standard error for three trees.

Some models (e.g. Williams et al., 1996) have overcome the former limitation by including an algorithm for determining Ψ_{leaf} based on previous amounts of water loss and cell elasticity. However, for the purpose of modelling the relative impacts of *P. gaeumannii* on needle physiology this is not necessary. Overall, our model was well correlated with observed values of stomatal conductance, and shows the impact of *P. gaeumannii* infection on g_s. For example, Fig. 6 compares the diurnal patterns of g_s on a typical day from a healthy and diseased tree at a high-disease site (Beaver-south). Also evident in Fig. 6 is the limitation imposed on maximum (i.e. early morning) g_s by *P. gaeumannii* infection.

Similar to g_s, our estimates of A_{net} were significantly correlated with observed values ($r^2 = 0.792$), again with a slight underestimation (slope = 0.820) (Fig. 7). The observed time-lag and over-estimation of early morning values were not as apparent for A_{net} estimates (Fig. 8) as compared to those for g_s. Fig. 8 shows a typical diurnal curve for three age classes of needles with no *P. gaeumannii* infection from a low-disease site (Mac-north). For this, and all days measured, a significant difference in maximum A_{net} between needle age classes was detected for needles from the high- (Beaver) and moderate-disease (Hebo) sites but not the low-disease site (Mac) (Table 1). The association

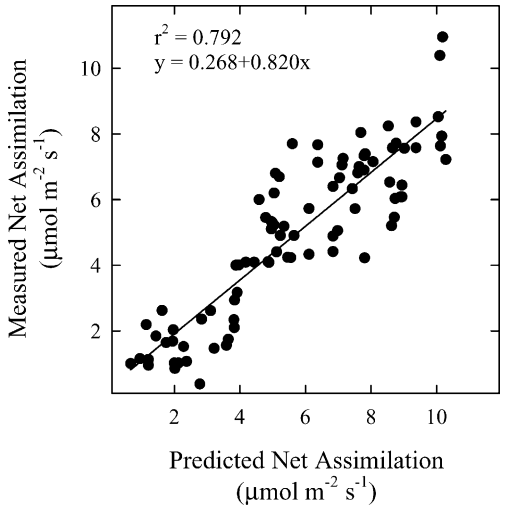

Fig. 7. Measured vs. predicted rates of net CO_2 assimilation (A_{net}) for current year, 1-, and 2-year-old needles with varying levels of *P. gaeumannii* infection (PD ranged from 0 to 61%) from three western Oregon Douglas-fir plantations. Each observation is the mean of six trees ($n = 89$) measured in 1999.

between maximum A_{net} and *P. gaeumannii* colonisation levels suggests that *P. gaeumannii* can be an important regulator of A_{net} as needles age. Furthermore,

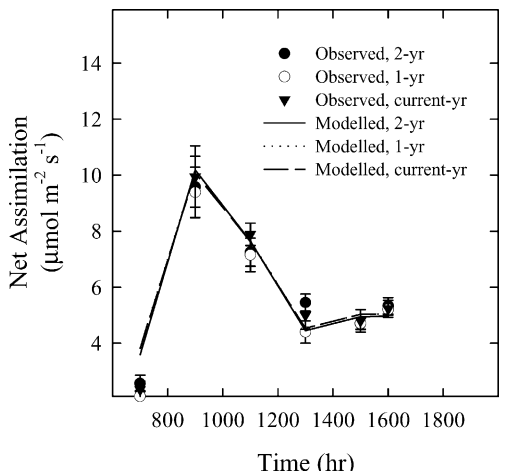

Fig. 8. Diurnal pattern of measured and predicted rates of net CO_2 assimilation (A_{net}) for sprayed current year, 1- and 2-year-old needles (mean PD was 0, 0 and 4%, respectively) from the low-disease site (Mac-north) on 4 August 1998. Each observation is the mean and standard error for three trees.

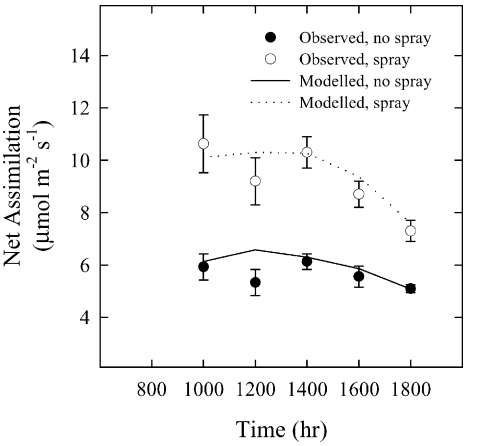

Fig. 9. Diurnal pattern of measured and predicted rates of net CO_2 assimilation (A_{net}) for sprayed (mean pseudothecia density was 0%) and un-sprayed (mean PD was 15%) 1-year-old needles from the high-disease site (Beaver-south) on 7 August 1998. Each observation is the mean and standard error for three trees.

unlike other studies (e.g. Jach and Ceulemans, 2000), changes in maximum A_{net} as needles aged were not correlated with foliar nitrogen concentrations (Fig. 2).

A decline in A_{net} due to *P. gaeumannii* infection was also present, with a good fit to the diurnal patterns of measured and observed values. Like g_s, diurnal rates of A_{net} were significantly reduced in diseased versus healthy trees, as shown for the high-disease site (Beaver-south) in Fig. 9.

2.5. Sensitivity analysis

We tested the effect of *P. gaeumannii* infection on model estimates by calculating g_s and A_{net} for a typical summer day (minimum/maximum values over the 24-hr simulation period were as follows: air temperature 12.9/29.8 °C, relative humidity 60/100%, PPFD 0/1356 mmol m^{-2} s^{-1}, and VPD 159/2161 Pa) over the range of observed PD and K_L values (Fig. 10). The first model run was conducted with PD levels ranging from 0 to 50% and K_L held constant at 0.11 mmol m^{-2} s^{-1} MPa^{-1} (Fig. 10A); the second run was conducted with K_L values ranging from 0.13 to 0.05 mmol m^{-2} s^{-1} MPa^{-1} and PD held constant at 0.0% (Fig. 10B). As shown, changes in PD had a much greater impact on gas exchange estimates. For example, over the range of PD values, g_s and A_{net} changed by 84.1 and 111.5%, respectively; and over

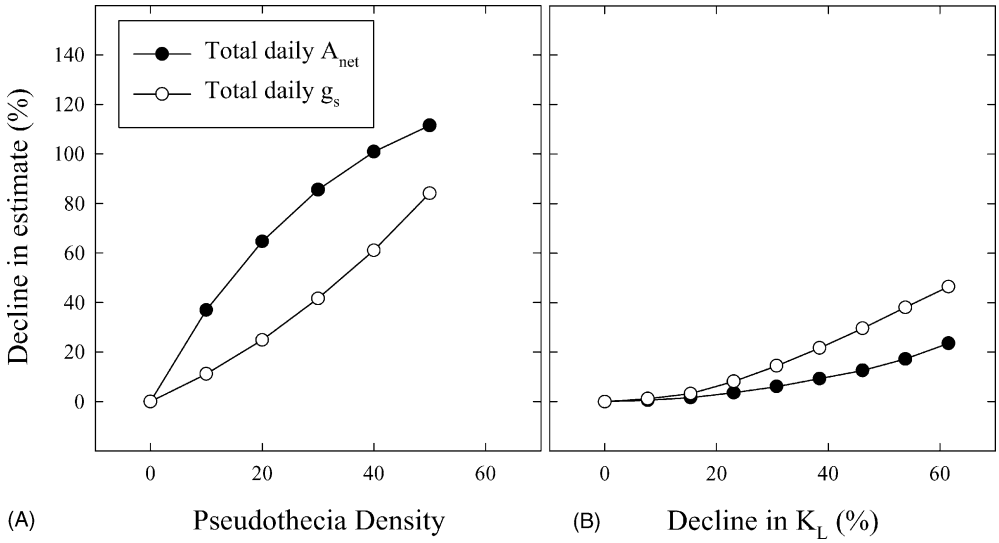

Fig. 10. Relationship between the percent decline in total daily stomatal conductance (g_s) and net CO_2 assimilation (A_{net}) estimates and increasing PD (panel A) or declining leaf-specific hydraulic conductance (K_L) (panel B).

the range of K_L values, g_s and A_{net} changed by only 46.5 and 23.6%, respectively.

3. Model simulation

As stated previously, the second objective of this study was to determine if *P. gaeumannii*'s impact on gas exchange is correlated with current growth losses in coastal Oregon Douglas-fir plantations. To determine this, branch-level estimates of A_{net} were scaled up over time and space and compared against observed volume growth for the same time period.

3.1. Study sites

Long-term estimates of whole-canopy A_{net} were calculated using the model for the sprayed and un-sprayed trees on each of the north and south plots from the three Douglas-fir plantations as follows. For each hour over a 10-month sample period (1 July 1998–30 April 1999), estimates of g_s and A_{net} were calculated for needles from each age class using plot-specific values of climate data (temperature, RH, PPFD, VPD, data not shown), and needle age class-specific values of PD (Table 2), and K_L (Table 3). A_{net} estimates were integrated over time by multiplying the sum of each hourly measurement for the 10-month period by $3600\,s\,h^{-1}$. Estimates were also scaled-up to a canopy estimate by multiplying by the whole-tree leaf area (m^2).

3.2. Whole-canopy scaling

Various techniques have been proposed to estimate whole-tree leaf areas (McDowell et al., 2002). However, in this case the best method should be easily parameterised, account for temporal changes in leaf area caused by *P. gaeumannii*-induced needle abscission, and be able to predict the relative leaf areas of all needle age classes present. Therefore, an allometric equation relating cross-sectional sapwood area (cm^2) and leaf area (m^2), for each of the youngest four needle age classes, was determined using healthy trees with full needle complements (i.e. 100% needle retention), and modifying these estimates in modelled trees (i.e. varying levels of *P. gaeumannii*-induced needle abscission) using visual estimates of needle retention (0–1) as follows.

One 5-year-old branch from each of the 12 healthy Mac forest trees was harvested in September 2000 for leaf area and branch diameter determinations. The leaf area for each age class (LA_x, where x denotes age class) was determined by multiplying the total

Table 2
PD (%) and needle retention (NR, %) values for each needle age class input into model

Site code[a]	Date[b]	PD				NR			
		3-year-old	2-year-old	1-year-old	Current year	3-year-old	2-year-old	1-year-old	Current year
BNNS	7-11	–	63.0	50.7	0.0	0.0	30.1	91.2	100
BNNS	12-4	–	76.6	64.7	4.8	0.0	28.6	91.0	100
BNS	7-11	–	41.3	29.2	0.0	0.0	53.4	77.1	100
BNS	12-4	–	53.8	33.2	0.1	0.0	51.1	76.8	100
BSNS	7-11	–	–	54.5	0.0	0.0	0.0	60.5	100
BSNS	12-4	–	–	66.4	18.7	0.0	0.0	60.5	100
BSS	7-11	–	–	24.2	0.0	0.0	0.0	77.1	100
BSS	12-4	–	–	47.5	0.1	0.0	0.0	76.8	100
HNNS	7-11	–	12.2	3.6	0.0	0.0	65.8	100	100
HNNS	12-4	–	16.8	17.0	2.7	0.0	64.2	98.2	100
HNS	7-11	–	4.5	4.0	0.0	0.0	84.2	100	100
HNS	12-4	–	20.4	6.8	0.3	0.0	84	99.5	100
HSNS	7-11	–	21.3	7.2	0.0	0.0	24.2	83.3	100
HSNS	12-4	–	55.3	29.5	0.0	0.0	22.2	82.1	100
HSS	7-11	–	19.0	4.7	0.0	0.0	46.1	85.7	100
HSS	12-4	–	35.8	15.0	0.5	0.0	43.1	86	100
MNNS	7-11	2.0	1.7	2.8	0.0	100	100	100	100
MNNS	12-4	10.7	10.7	27.7	0.6	100	100	100	100
MNS	7-11	1.0	0.9	6.4	0.0	100	100	100	100
MNS	12-4	4.5	4.5	9.7	0.4	100	100	100	100
MSNS	7-11	0.5	0.2	2.7	0.0	100	100	100	100
MSNS	12-4	1.3	1.3	16.5	1.0	100	100	100	100
MSS	7-11	0.9	0.9	3.8	0.0	100	100	100	100
MSS	12-4	2.2	2.2	3.4	0.0	100	100	100	100

[a] The first letter corresponds to the site (B, Beaver, H, Hebo, M, Mac), the second letter is the slope (N, north, S, south), and the third and fourth letters are the spray treatment (NS, no spray, S, spray).
[b] Date is the month(s) of the year modelled using the listed values (7-11: July 1998–November 1998, 12-4: December 1998–April 1999).

Table 3
Values of the percent of latewood present in sapwood (LW, %) input into model

Site code[a]	LW[b]
BNNS	63
BNS	42
BSNS	62
BSS	36
HNNS	32
HNS	25
HSNS	33
HSS	28
MNNS	35
MNS	38
MSNS	38
MSS	31

[a] The first letter corresponds to the site (B, Beaver, H, Hebo, M, Mac), the second letter is the slope (N, north, S, south), and the third and fourth letters are the spray treatment (NS, no spray, S, spray).
[b] Reported values for each site code were used for all needle age classes and months modelled.

leaf dry weight present on the branch by a projected leaf area to dry weight ratio determined from a random sub-sample of 100 needles from each branch. These branch-level, leaf area determinations were used to create an allometric equation relating branch cross-sectional area (SA, at 5 cm from junction of main stem) and leaf area. The relationship between leaf area (LA_0, current year; LA_1, 1-year-old, etc.) and branch cross-sectional area for the four age classes are as follows:

$$LA_0 = 0.1965 \times SA, \quad r^2 = 0.8614 \tag{17}$$

$$LA_1 = 0.1497 \times SA, \quad r^2 = 0.9039 \tag{18}$$

$$LA_2 = 0.0528 \times SA, \quad r^2 = 0.8257 \tag{19}$$

$$LA_3 = 0.0055 \times SA, \quad r^2 = 0.2186 \tag{20}$$

A whole-tree estimate of leaf area for each age class (TLA_x) was calculated by measuring diameters of all living branches on each tree and summing the

estimates of LA_x. The whole-tree leaf area (TLA) is the sum of TLA_x for all needle age classes. Similar to other studies (McDowell et al., 2002), a consistent linear relationship between stem diameter at breast height (DBH) and estimates of TLA was observed:

$$TLA = 0.4045 \times DBH, \quad r^2 = 0.8983 \qquad (21)$$

Finally, the relative distribution of the needle age classes for the whole-tree ($RLA_x = TLA_x/TLA$) was determined to be 47.1 ± 1.5%, 36.4 ± 1.4%, 14.2 ± 0.9%, and 2.3 ± 0.4% for the current year, 1-, 2-, and 3-year-old needles, respectively. From the above calculations, whole-tree TLA_x for all modelled trees was estimated by Eqs. (21) and (22):

$$TLA_x = TLA \times RLA_x \times NR_x, \qquad (22)$$

which could be estimated at any point in time from only DBH and needle retention (NR_x) measurements. Estimates of leaf areas derived from Eq. (22) were

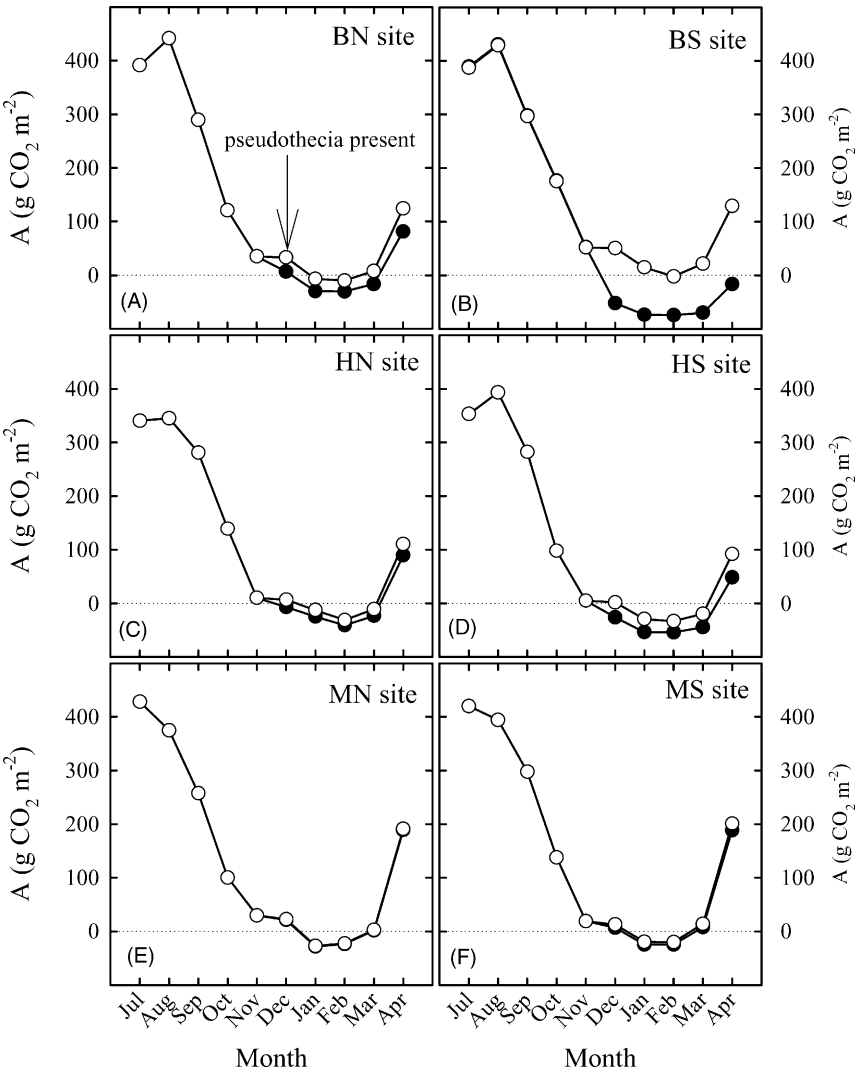

Fig. 11. Modelled total monthly value of net CO_2 assimilation (A_{net}) per unit leaf area for the no spray or diseased (closed symbols) and sprayed or healthy (open symbols) current year needles. The first letter of the site code is the site (B, Beaver, H, Hebo, M, Mac), and the second letter is the slope (N, north, S, south).

verified by determining estimates of TLA_x, using the same methods outlined for the Mac trees above, for three diseased trees from the Beaver site. All estimates of TLA_x computed by the two methods were within 5% of each other (data not shown).

3.3. Volume growth data

An index of tree volume growth was calculated as the product of the following height and area growth measurements. In May 2000, height growth in all modelled trees was estimated by measuring the length of the 1999 internode on the main stem. Diameter growth was estimated for the same year by calculating the area of the sapwood ring, whose average radius was determined from two increment cores (north and west aspect) taken at 1.4 m above the ground.

4. Results

The pattern of gas exchange for current year needles over time is shown in Fig. 11. A_{net} was highest in the summer (reaching values of ca. 400 g CO_2 m^{-2} LA) and declined in the winter to near or below zero. After November, when pseudothecia emerged from needle stomata, A_{net} in the sprayed and un-sprayed trees diverged, and at the site with the highest levels of *P. gaeumannii* colonisation (Beaver-south plot) April 1999 values of A_{net} were ca. 150 and 0 g CO_2 m^{-2} LA for the sprayed and un-sprayed needles, respectively.

Estimates of the long-term carbon budgets in needles with varying levels of *P. gaeumannii* show that once infection levels were high enough, needles became a sink for carbon. Fig. 12A shows A_{net} estimates for each age class of needles from all six plots plotted against the amount of *P. gaeumannii* colonisation (pseudothecia density). Despite differences in climate, the relationship is highly significant over the 10-month simulation period, and once pseudothecia density increases above ca. 25%, carbon budgets become negative. Fig. 12B shows the relationship between A_{net} and observed needle retentions the following spring (April 2000). Based on this plot, needle retention decreased linearly as A_{net} decreased, and all needle age classes that were carbon sinks had been completely abscised by the spring of 2000.

When scaled to the canopy level all modelled trees were estimated to have positive carbon budgets (Table 4). Current year needles were the largest contributors to the carbon gain of all trees, and at the high-disease plots (Beaver) they were the only needle age class with positive carbon budgets. The relationship between the estimated whole-canopy A_{net} and

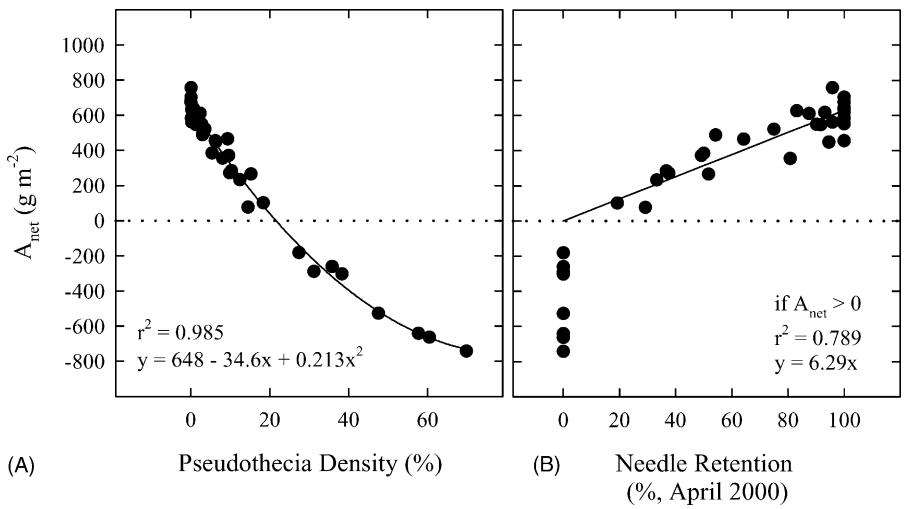

Fig. 12. Total long-term estimate of net CO_2 assimilation (A_{net}) per unit leaf area in relationship to [panel A] *P. gaeumannii* pseudothecia density (%) or [panel B] needle retention (%, April 2000). A_{net} is the modelled value for each needle age class present within a plot; pseudothecia density is the average percentage of stomata with visible pseudothecia from six trees.

Table 4
Total net CO_2 assimilation (A_{net}, kg) for each needle age class over the entire 10-month simulation

Age	BNNS[a]	BNS	BSNS	BSS
3-year-old	–	–	–	–
2-year-old	−2.7	−2.6	–	–
1-year-old	−14.7	−9.2	−6.9	−4.3
Current year	21.5	33.2	12.1	27.9
Total	4.2	21.3	5.2	23.7
	HNNS	HNS	HSNS	HSS
3-year-old	–	–	–	–
2-year-old	0.7	2.7	−1.2	−0.9
1-year-old	8.4	14.0	1.9	6.1
Current year	21.3	28.0	14.9	20.6
Total	30.4	44.7	15.6	26.2
	MNNS	MNS	MSNS	MSS
3-year-old	0.4	0.6	0.6	0.7
2-year-old	4.2	5.7	6.1	6.6
1-year-old	7.1	10.2	10.3	15.8
Current year	21.4	24.0	22.9	27.0
Total	33.1	40.5	39.9	50.1

[a] The first letter corresponds to the site (B, Beaver, H, Hebo, M, Mac), the second letter is the slope (N, north, S, south), and the third and fourth letters are the spray treatment (NS, no spray, S, spray). Missing values are due to needle abscission. Corresponding *P. gaeumannii* infection levels are in Table 2.

volume growth rates was assessed by regression analysis (Fig. 13). Across all plots, a significant linear relationship was found ($r^2 = 0.683$).

Fig. 14 shows the results of different model runs to determine the relative influence of reduced gas exchange rates per unit LA or reduced needle retention (i.e. needle abscission) on whole-canopy A_{net}. For each site, four different estimates of whole-canopy A_{net} were calculated over the 10-month simulation. These included: (i) the maximum possible A_{net} or when needle retention (NR) was set to 100% and pseudothecia density (PD) was set to 0%, (ii) the impact of needle retention, i.e. actual NR values (Table 2) with PD set to 0%, (iii) the impact of PD, i.e. actual PD values (Table 2) with NR set to 100%, and (iv) the impact of NR and PD, i.e. actual PD and NR values (Table 2). The values reported in Fig. 14 are the percent decline in the three latter simulations (ii–iv) from the maximum (i). Overall, the impact of *P. gaeumannii* on needle gas exchange rates had a large influence on

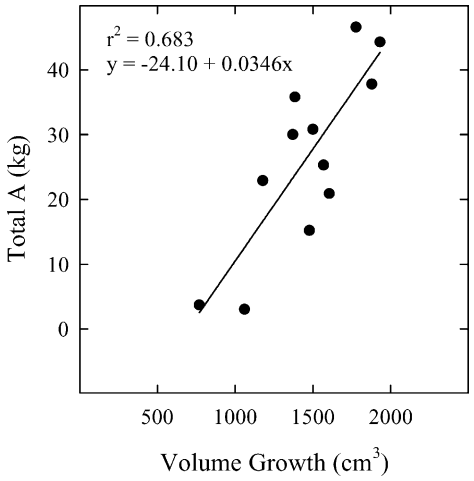

Fig. 13. Total long-term estimate of net CO_2 assimilation (A_{net}) vs. volume growth. Growth parameters are the mean of six disease or six un-diseased trees from each site.

whole-canopy A_{net}. For example, at the Beaver-south plot, *P. gaeumannii*'s impact on gas exchange rates reduced A_{net} by 110.6%; whereas, needle abscission and the loss of leaf area, assumed to be disease-free,

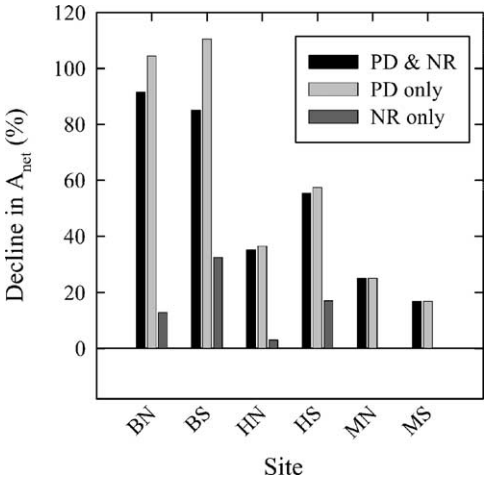

Fig. 14. Percent change in the estimate of long-term net CO_2 assimilation (A_{net}) due to various disease components as compared to a model run with 100% needle retention (NR) and 0% PD. Bars are as follows: NR only compares actual and 100% NR both at 0% PD, PD only compares actual and 0% PD both at 100% NR and NR and PD compares actual PD and NR with 0% PD and 100% NR. The first letter of the site code is the site (B, Beaver, H, Hebo, M, Mac), and the second letter is the plot-aspect (N, north, S, south).

reduced A_{net} by only 32.6%. In reality, however, because the abscised needles had high levels of *P. gaeumannii* infection and negative carbon budgets (i.e. not disease-free as assumed in simulation ii), their abscission mitigated the decline in whole-canopy A_{net} such that the effect of *P. gaeumannii* on whole-canopy A_{net} declined to 85.1%.

5. Discussion

The colonisation of Douglas-fir needles by *P. gaeumannii* begins in early summer when newly emerging needles are infected by deposited ascospores (Hansen and Lewis, 1997). Colonisation of needles increases over time with the emergence of pseudothecia from stomata 1–4 years later (Hansen et al., 2000). Gaseous diffusion of CO_2 and H_2O is physically impaired by these fungal structures (Manter et al., 2000) and beginning in December, when pseudothecia emerged from stomata, A_{net} rates in diseased foliage are significantly reduced compared to healthy foliage.

It has been hypothesised that needle abscission begins when needles switch from being a carbon source to a carbon sink (McMurtrie et al., 1986; Cannell and Morgan, 1990). In a healthy plant, the foliar carbon budget is largely attributed to local photosynthetic rates, since mature needles import little photosynthate and respiration rates are low relative to assimilation (Sprugel et al., 1991), and nutrient content (Balster and Marshall, 2000). Two primary factors have been hypothesised to account for the decline in A_{net} of older needles: reduced light (Schoettle and Smith, 1991) and nutrient (Balster and Marshall, 2000) content. Our data demonstrate a third cause, fungal-mediated occlusion of stomata and declines in gas exchange. From our estimated carbon budgets, once approximately 25% of needle stomata contain visible *P. gaeumannii* pseudothecia needles become carbon sinks. Although these needles can still actively photosynthesize during daylight hours (Manter et al., 2000), their respiration costs result in a net negative carbon balance for the year. Previous studies at the same sites used in this modelling exercise have shown that needle abscission first begins when the 25% needle colonisation level is reached (D.K. Manter, unpublished data), suggesting that needle longevity is related to carbon budgets; and a later survey (April 2000) showed that all unproductive needle age classes had been completely abscised.

All of the carbon required for plant growth is acquired through photosynthesis; therefore, if whole-canopy A_{net} and leaf area can be measured then the amount of carbon available for growth can be estimated (e.g. Ledig, 1969). We assessed the relationship between volume growth and long-term estimates of whole-canopy A_{net}. Despite the presence of *P. gaeumannii*, canopy carbon budgets of all modelled trees remained positive due to the large contribution of current year needles to the total canopy carbon budget. When *P. gaeumannii* colonisation was limited by fungicide applications, carbon budgets and volume growth increased; and at all plots, a single positive linear relationship between modelled whole-canopy A_{net} and volume growth was found.

At the landscape level, fungal leaf colonists such as *P. gaeumannii* may have a profound effect on net CO_2 assimilation of forest canopies. For example, based on our estimates, the reported 23–50% decline in volume growth of *P. gaeumannii*-infected coastal Oregon Douglas-fir trees (Maguire et al., 2002) would be equivalent to a reduction in whole-canopy A_{net} of 15.9–34.6 kg CO_2 tree^{-1} year^{-1} (as compared to a healthy tree with an annual volume growth of 2000 cm^3). For the entire 119,500 ha of coastal Oregon forest plantations exhibiting SNC symptoms, total A_{net} would be reduced by ca. 0.5–1 million metric tons (assuming 250 trees ha^{-1}). Furthermore, this massive reduction in carbon fixation is: (i) accomplished by a fungus whose biomass constitutes less than 2.5% of the total foliar biomass in a heavily infected tree (0.11 kg DW of *P. gaeumannii* and 4.7 kg DW of LA per tree at the Beaver-south site; D.K. Manter, unpublished data), and (ii) equivalent to ca. 7.7–15.4% of the 6.5 million metric tons of CO_2 emitted from Oregon's power plants in 1999 (US Department of Energy, 1999).

This paper documents the limitations on whole-canopy A_{net}, and its significant relationship to growth, imposed by the native Douglas-fir pathogen, *P. gaeumannii*, in Oregon forests. The cause of the recent intensification of SNC in the PNW is unknown; however, *P. gaeumannii* is widespread in both natural and managed stands of Douglas-fir. Because of Douglas-fir's high wood quality and productivity, approximately 1 million ha of plantations are currently in production

world-wide, in addition to the 14.3 million ha in the United States (Hermann and Lavender, 1999). Normally, the latent period of *P. gaeumannii* lasts several years, and fungal fruiting occurs primarily on the 3-year-old and older needles. Under these conditions, *P. gaeumannii* would remain a minor factor in limiting Douglas-fir forest productivity since ca. 85% of whole-canopy A_{net} occurs in the current and 1-year-old needles. Alternatively, in regions where faster *P. gaeumannii* colonisation rates occur (current year and 1-year-old needles with greater than 25% of stomata with visible *P. gaeumannii* pseudothecia) selection of Douglas-fir genotypes with shorter needle longevities should increase forest productivity by removal of the diseased needles that are a net drain on whole-canopy A_{net} and growth. However, since the overwhelming impact of *P. gaeumannii* is on gas exchange, as long as, *P. gaeumannii* is present and reaches sexual maturity (i.e. produces pseudothecia), significant declines in whole-canopy A_{net} and growth will continue.

Acknowledgements

This research was funded through the Swiss Needle Cast Cooperative at Oregon State University—a consortium of industrial, federal, tribal, and state landowners in Oregon and Washington.

References

Balster, N.J., Marshall, J.D., 2000. Decreased needle longevity of fertilized Douglas-fir and grand fir in the northern Rockies. Tree Physiol. 20, 1191–1197.

Bond, B.J., Kavanagh, K.L., 1999. Stomatal behavior of four woody species in relation to leaf specific hydraulic conductance and threshold water potential. Tree Physiol. 19, 503–510.

Boyce, J.S., 1940. A Needle-cast of Douglas-fir in New Zealand. Forest Research Institute, Rotorua, New Zealand. FRI Symposium No. 15.

Cannell, M.G.R., Morgan, J., 1990. Theoretical study of variables affecting the export of assimilates from branches of *Picea*. Tree Physiol. 6, 257–266.

Dewar, R.C., 1995. Interpretation of an empirical model for stomatal conductance in terms of guard cell function. Plant Cell Environ. 18, 365–372.

Farquhar, G.D., von Caemmerer, S., Berry, J.A., 1980. A biochemical model of photosynthetic CO_2 assimilation in leaves of C_3 species. Planta 149, 78–90.

Hansen, E.M., Lewis, K.J., 1997. Compendium of Conifer Diseases. APS Press, St. Paul, MN, USA.

Hansen, E.M., Stone, J.K., Capitano, B.R., Rosso, P., Sutton, W., Winton, L., Kanaskie, A., McWilliams, M.G., 2000. Incidence and impacts of Swiss needle cast in forest plantations of Douglas-fir in coastal Oregon. Plant Dis. 84, 773–778.

Harley, P.C., Thomas, R.B., Reynolds, J.F., Strain, B.R., 1992. Modelling photosynthesis of cotton grown in elevated CO_2. Plant Cell Environ. 15, 271–282.

Hermann, R.K., Lavender, D.P., 1999. Douglas-fir planted forests. New For. 17, 53–70.

Hood, I.A., 1982. *Phaeocryptopus gaeumannii* on *Pseudotsuga menziesii* in southern British Columbia. N. Z. J. For. Sci. 2, 415–424.

Jach, M.E., Ceulemans, R., 2000. Effects of season, needle age and elevated atmospheric CO_2 on photosynthesis in Scots pine (*Pinus sylvestris*). Tree Physiol. 20, 45–157.

Jones, H.G., Sutherland, R.A., 1991. Stomatal control of xylem embolism. Plant Cell Environ. 14, 607–612.

Jordan, D.B., Ogren, W.L., 1984. The CO_2/O_2 specificity of ribulose 1,5-bisphosphate carboxylase/oxygenase: dependence on ribulose-bisphosphate concentration, pH and temperature. Planta 161, 308–313.

Ledig, F.T., 1969. A growth model for tree seedlings based on the rate of photosynthesis and the distribution of photosynthate. Photosynthetica 3, 263–275.

Leverenz, J.W., 1981. Photosynthesis and transpiration in large forest-grown Douglas-fir: diurnal variation. Can. J. Bot. 59, 349–356.

Maguire, D.A., Kanaskie, A., Voelker, W., Johnson, R., Johnson, G., 2002. Growth of young Douglas-fir plantations across a gradient in Swiss needle cast severity. West. J. Appl. For. 17, 86–95.

Manter, D.K., Bond, B.J., Kavanagh, K.L., Rosso, P.H., Filip, G.M., 2000. Pseudothecia of Swiss needle cast fungus, *Phaeocryptopus gaeumannii*, physically block stomata of Douglas fir, reducing CO_2 assimilation. New Phytol. 148, 481–491.

McDowell, N.G., Barnard, H., Bond, B.J., Hinckley, T., Hubbard, R., Ishii, H., Kostner, B., Meinzer, F.C., Marshall, J.D., Marshall, F., Magnani, F., Phillips, N., Ryan, M.G., Whitehead, D., 2002. The relationship between tree height and leaf area:sapwood area ratio. Oecologia 132, 12–20.

McMurtrie, R.E., 1993. Modelling of canopy carbon and water balance. In: Hall, D.O., Scurlock, J.M.O., Bolhar-Nordenkampf, H.R., Leegood, R.C., Long, S.P. (Eds.), Photosynthesis and Production in a Changing Environment: A Field and Laboratory Manual. Chapman and Hall, London, pp. 220–231.

McMurtrie, R.E., Linder, S., Benson, M.L., Wolf, L., 1986. A model of leaf area development for pine stands. In: Fujimori, T., Whitehead, D. (Eds.), Crown and Canopy Structure in Relation to Productivity. Forestry and Forest Products Research Institute, Ibaraki, Japan, pp. 284–307.

Schoettle, A.W., Smith, W.K., 1991. Interrelation between shoot characteristics and solar irradiance in the crown of *Pinus contorta* spp. *Latifolia*. Tree Physiol. 9, 245–254.

Sprugel, D.G., Hinckley, T.M., Schaap, W., 1991. The theory and practice of branch autonomy. Ann. Rev. Ecol. Syst. 22, 309–334.

US Department of Energy, 1999. State electricity profiles, DOE/EIA-0629. Energy Information Administration, Office of Coal, Nuclear, Electricity and Alternative Fuels, Washington, DC.

Webb, W.L., 1991. Atmospheric CO_2, climate change, and tree growth: a process model. I. Model structure. Ecol. Model. 56, 81–107.

Whitehead, D., 1998. Regulation of stomatal conductance and transpiration in forest canopies. Tree Physiol. 18, 633–644.

Williams, M., Rasletter, E.B., Fernandes, D.N., Goulden, M.L., Wofsy, S.C., Shaver, G.R., Melillo, J.M., Munger, J.W., Fan, S.-M., Nadelhoffer, K.J., 1996. Modelling the soil–plant–atmosphere continuum in a Quercus-Acer stand at Harvard Forest: the regulation of stomatal conductance by light, nitrogen and soil/plant hydraulic. Plant Cell Environ. 19, 911–927.

Wullschleger, S.D., 1993. Biochemical limitations to carbon assimilation in C_3 plants—a retrospective analysis of the A/C_i curves from 109 species. J. Exp. Bot. 44, 907–920.